

## Breakdown Directions in Lithium Halide Crystals\*

J. W. DAVISSON\*\*

*Laboratory for Insulation Research, Massachusetts Institute of Technology, Cambridge, Massachusetts*

(Received January 22, 1948)

Electrical breakdown paths in the lithium halide crystals form star patterns consisting of 12 paths of the type  $[xxy]$  where  $x \geq y$ . The paths lie within the acute sectors of the (110) planes bounded by the directions  $[110]$  and  $[111]$ .

The star assumes the  $[110]$  orientation at low temperatures and tends to approach the  $[111]$  position as the temperature increases. Under overvoltage conditions, complex  $[xxy]$  patterns are obtained; they show abrupt changes in orientation as the paths proceed through the crystal, but follow a definite sequence of directions.

It is shown that, although the breakdown paths seem to mark those directions in which electrons can be accelerated most rapidly to the ionization potential of the lattice, the star paths apparently do not follow simply from an electron wave interaction with the lattice or from a statistical competition between breakdown in the  $[110]$  and  $[111]$  directions.

### I. INTRODUCTION

IT has been shown<sup>1</sup> that lithium halide crystals undergo electric breakdown in the directions  $[xxy]$  at elevated temperatures, and that the parameters  $x$  and  $y$  may be temperature dependent. The present, more detailed investigation of the star patterns and a comparison with the breakdown paths obtained in other crystals give further insight into the mechanism of electrical breakdown.

### II. CRYSTALS

The alkali halide crystals used in the following experiments were, in general, grown from the melt. Pure LiF crystals were obtained commercially.\*\*\* CsCl and NaClO<sub>3</sub> crystals were grown by slow evaporation of the aqueous solution. LiI crystals could not be obtained because the material decomposes readily at its melting temperature.

### III. APPARATUS AND PROCEDURE

A crystal section about 1 sq. cm in area and 10 mils in thickness was placed between a metallic point-plane electrode system and im-

mersed in an insulating medium which forced the breakdown to take place through the crystal instead of in the air over its surface. To yield paths that lie close to the surface and to limit the current at breakdown to such small values that fracturing is avoided, a glass microscope slide, which served as a series resistance, was inserted between the crystal and the plane electrode. With liquid insulating media, which were used up to 450°C (the boiling point of sulfur), each crystal section was subjected to numerous breakdowns of (+) and (-) polarity by shifting the point electrode. Above 450°C the crystals were heated in vacuum by radiation from an electric oven (Fig. 1).

In the previous study<sup>1</sup> breakdown was effected by means of a high frequency spark discharge; hence the breakdown voltage was not known in magnitude or sign. For the present investigation a high voltage source was used which produced a pulse of known sign and rise time and a roughly controllable magnitude.† A 4- $\mu$ f condenser, charged up to 600 volts, was discharged through the primary of an induction coil by means of a thyatron. The high voltage pulse of 50 kv max. and  $(10)^{-5}$  sec. front was rectified by means of a kenotron. Direct current breakdown tests were performed with a 50-kv voltage supply consisting of a conventional voltage doubler circuit with accompanying filters.

\* This research was made possible through support extended to the Massachusetts Institute of Technology, Laboratory for Insulation Research, jointly by the Navy Department (Office of Naval Research) and the Army Signal Corps under ONR Contract N5-ori-78, T.O.I.

\*\* Present address, Crystal Section, Naval Research Laboratory, Washington, D. C.

<sup>1</sup> J. W. Davison, Phys. Rev. **70**, 685 (1946).

\*\*\* The Harshaw Chemical Company, Cleveland, Ohio.

† This unit was designed by D. Young, Laboratory for Insulation Research, Massachusetts Institute of Technology.

IV. GEOMETRICAL CONSIDERATIONS AND OPTICAL MEASUREMENTS

The directions assumed by electrical breakdown paths in the lithium halide crystals may be represented in terms of zonal parameters  $[uvw]$  by the indices  $[xxy]$  where  $x \geq y$ . (The zonal parameters are the components of the path in the directions of the coordinate axes, that is, in the cube edge directions of Fig. 2.) The double indices  $xx$  require that the paths lie within the (110) planes, while the restriction  $x \geq y$  shows that they are confined to the acute sectors of the (110) planes bounded by the directions  $[110]$  and  $[111]$ . The indices of the 12 paths, which comprise a complete  $[xxy]$  star pattern, are, according to macroscopic symmetry:

$\underline{xxy}$	$\underline{xx\bar{y}}$	$\underline{x\bar{x}y}$	$\underline{\bar{x}xy}$
$\underline{xyx}$	$\underline{xy\bar{x}}$	$\underline{x\bar{y}x}$	$\underline{\bar{y}yx}$
$\underline{yxx}$	$\underline{yxx}$	$\underline{y\bar{x}x}$	$\underline{\bar{y}xx}$

where the bar means that the designated index is negative and the underscore signifies that the same path directions represented by indices with negative signs are included.

The pattern may be visualized as follows (Fig. 2): from the midpoint (0) of a (001) cube face four  $[110]$  face-diagonal directions are obtained by joining (0) with the midpoints  $P, Q, R,$  and  $S$  of the vertical cube faces. The two additional  $[110]$  directions are given by the surface diagonals  $U-U'$  and  $V-V'$  which intersect at (0). The four  $[111]$  body diagonals result by joining (0) with the midpoints  $W, X, Y,$  and  $Z$  of the vertical cube edges. The (110) planes, determined by any two intersecting  $[111]$  directions, are of two types: two vertical planes  $WUUY$  and  $XVV'F'$  and four oblique planes  $OWX, OXY, OYZ,$  and  $OZW$ . The direction of a star path, since it lies within a (110) plane, may be specified by its deviation  $\alpha$  from a  $[110]$  direction. A star pattern of given deviation  $\alpha$ , centered at (0), consists of 12 paths directed towards  $A, A', B, B', C, C', D, D', E, E', F,$  and  $F'$ . The four paths from (0) to  $E, E', F,$  and  $F'$  make a larger inclination angle with the vertical than the eight remaining paths. In terms of path indices the 4 paths from (0) to  $E, E', F,$  and  $F'$  are of the type  $[xxy]$  and the eight

remaining paths are of the types  $[xyx]$  and  $[yxx]$ .

The star patterns, once it has been established that their loci are the (110) planes,†† are completely determined geometrically by the projection of their paths upon the cube face (Fig. 3). For all values of  $\alpha$  the four paths from (0) to  $E, E', F,$  and  $F'$  will always project into the  $45^\circ$  lines and will hereafter be referred to as diagonal paths. The eight remaining paths, the "off-diagonal paths," however, will vary in azimuth  $\phi$  from  $0^\circ$  to  $45^\circ$  as  $\alpha$  varies from  $0^\circ$  for  $[110]$  to  $35.6^\circ$  for the  $[111]$  orientation. (The deviation  $\alpha$  and the azimuth  $\phi$  are related by the expression  $\sqrt{2} \tan \alpha = \tan \phi$ .) It is apparent that the ratio  $y/x$ , which completely determines the geometry of the pattern, may be obtained directly from the projection figure by measuring the azimuth of the off-diagonal paths, since  $\tan \phi = y/x$ .

The breakdown paths obtained experimentally were examined under a stereomicroscope. Only those paths which showed no accompanying crystal fracture at  $100\times$  magnification were selected for measurement, unless otherwise stated. The azimuthal angle measurements were made with a petrographic microscope equipped with a translating and rotating stage. Although the azimuth is given relative to the cube edge directions, the diagonal breakdown paths in the  $45^\circ$  positions were actually used as the experimental datum lines. This choice was dictated by the fact that the face diagonals are projection

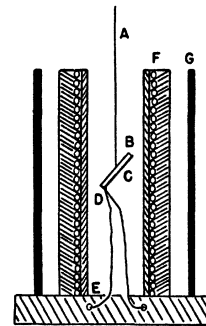


FIG. 1. Breakdown in vacuum. A is the high voltage electrode; B, crystal sample; C, Aquadag coating; D, Chromel-Alumel thermocouple fused to B; E, ceramic base plate; F,  $\frac{1}{2}$  in.- $\times$ 3 in.-cylindrical furnace; G, copper heat shield.

†† Twenty-four path directions would appear if they were not confined to reflection planes. Detailed measurements of typical star patterns are presented in reference 1.

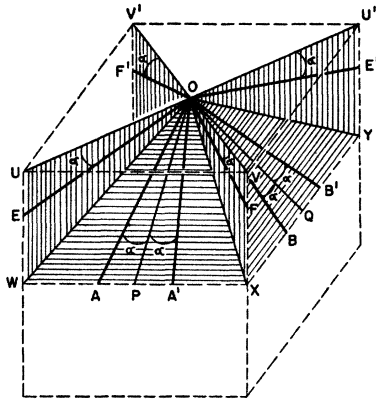


FIG. 2. Geometry of an [xxy] star pattern. The star paths are directed from (0) to A, A', B, B', C, C', D, D', E, E', F, and F'.

paths of the star patterns and are therefore easily identified.

The inclination angles of the paths were measured periodically to verify their [xxy] nature. The horizontal component of the path was obtained by means of a micrometer eyepiece while the vertical component was measured by the fine focus adjustment screw with allowance made for the index of refraction. The experimental error is about  $\pm 1^\circ$  for azimuth and  $\pm 3^\circ$  for the inclination angle.

V. RESULTS AT MINIMUM VOLTAGE

Lithium Fluoride

The orientation of breakdown paths in LiF as a function of temperature and polarity is shown

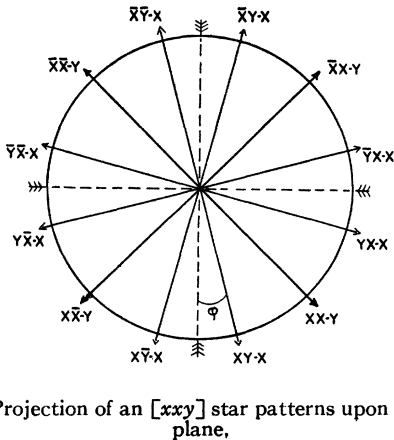


FIG. 3. Projection of an [xxy] star patterns upon the (001) plane,

in the projection diagrams of Fig. 4. The diagrams are to be read as follows: the individual dots and crosses are representative of the orientations observed for negative and positive breakdown paths respectively. The radial lines show the average negative breakdown directions.

The diagrams give the following information:

(4A) At  $-70^\circ\text{C}$  and below, only [110] paths are obtained with (-) and (+) d.c. and pulse voltages. The surface diagonals are not represented because [100] and not [110] surface paths were observed.

(4B) At  $0^\circ\text{C}$ , (-) pulses yield [110] paths and a star of azimuth  $10^\circ$ ; (+) pulses yield only [110] paths.

(4C) At  $25^\circ\text{C}$ , d.c. and pulse, (-) a  $13^\circ$  star and rarely [110] paths; (+) only [110] paths.

(4D) At  $50^\circ\text{C}$ , pulse, (-) a  $13^\circ$  star; (+) [110] paths.

(4E) At  $100^\circ\text{C}$ , pulse, (-) a  $15^\circ$  star; (+) [110] paths dominant with star paths appearing at various azimuths, which, however, are less than  $15^\circ$ .

(4F) At  $125^\circ\text{C}$ , pulse, (-) a  $15^\circ$  star; (+) [110] paths are no longer observed; a star of  $8^\circ$  with large individual variations in azimuth is found.

(4G) At  $150^\circ\text{C}$ , pulse, (-) a  $19^\circ$  star; (+) a  $16^\circ$  star. Under equilibrium d.c. conditions metallic dendrites are formed. (See below.)

(4H) At  $250^\circ\text{C}$ , pulse, for (-) and (+) a  $21^\circ$  star. Equilibrium d.c. yields dendrites, but with overvoltage star paths of  $21^\circ$  azimuth were obtained at  $235^\circ\text{C}$ .

(4I) At  $300^\circ\text{C}$ , a  $23^\circ$  star (Fig. 5). The crosses in Fig. 4I show the orientation obtained in the vacuum chamber (Fig. 1) and the dots, nearly coinciding, refer to breakdown observed with a liquid embedding medium.

(4J) At  $350^\circ\text{C}$  a  $25^\circ$  star for (-) and (+) pulse voltage.

(4K) At  $450^\circ\text{C}$ , pulse, (-) and (+) yield a star of azimuth  $26^\circ$ . Individual paths may attain azimuths as great as  $30^\circ$ . Even with a protective resistance [111] paths are frequently obtained especially with positive pulses. Only dendrites were obtained with d.c.

(4L) Above  $450^\circ\text{C}$  the breakdown paths behave as follows:

450°C	26° star and [111]
510	[111]
525	[111]
550	[111]
600	[110] and [111]
650	[110]
700	[110]
800	random

No difference in the physical appearance of the (+) and (-) patterns was observed. The paths are generally straight (Fig. 5) but those of the same orientation in a single specimen may not be strictly parallel. At 250°C, for example, the following set of azimuths was obtained: 18.6°, 21.5°, 20.5°, 21°, 21°, 18.5°, 19°, 19°, 21°, 18°, 20°, 19°, 18°, 19°, even though the individual paths were straight and showed no initial bending.

The influence of temperature was also similar for both polarities, but the positive patterns were retarded in azimuth with respect to the negative in the low temperature range. An increase of temperature in the range from 0°C to 450°C tended to shift the patterns towards [111]; a discontinuous jump from an azimuth of about 26° to 45° ([111] paths) seemed to occur near 450°C. The [111] paths appear between 450°C and 600°C, while above 600°C [110] paths were again observed. Complete star patterns most readily form between 200°C and 500°C, while at room temperature usually one or two paths appeared. Above 600°C stunted patterns similar to Fig. 6 were obtained.

Confirming von Hippel's conclusion<sup>2</sup> the same breakdown directions appeared in oblique crystal cuts. In (110) sections, for example, paths at four different angles of inclination were observed. Since a [110] direction is vertical, two paths deviated from the vertical by 13° at room temperature.

Results obtained in thin sections (2 to 3 mils) suggest that a thickness dependence of path orientation may exist. This was particularly noticeable at low temperatures. Under d.c. conditions at -170°C the paths in thick sections tended to start initially with large azimuths and to straighten out almost immediately into the

[110] direction. In thin sections, however, the initial change in azimuth took place more slowly with the result that the paths presented a curved aspect tending towards, but usually not attaining, the [110] direction.

### Lithium Chloride

The breakdown behavior of LiCl is shown in Fig. 7:

(7A) At -170°C, d.c. and pulse, (+) and (-), [110] paths dominant.

(7B) At 25°C, with overvoltage (see below), paths appear at all azimuths from 0° to 30°.

(7C) At 25°C, pulse, (-) a 10° star dominant; (+) [110] dominant.

(7D) At 100°C, pulse, (-) a 20° star; (+) a 15° star.

(7E) At 150°C, pulse, (-) and (+), azimuths ranging from 20° to 30°. Direct current yielded white metallic dendrites that lacked orientation.

(7F) At 200°C a star pattern of azimuth 30°.

(7G) At 300°C a path orientation was poor; path development extended only a short distance from the probe with maximum azimuth 30° (Fig. 6).

(7H) At 450°C, same as G but orientation is less definite.

The star patterns in LiCl shifted more rapidly

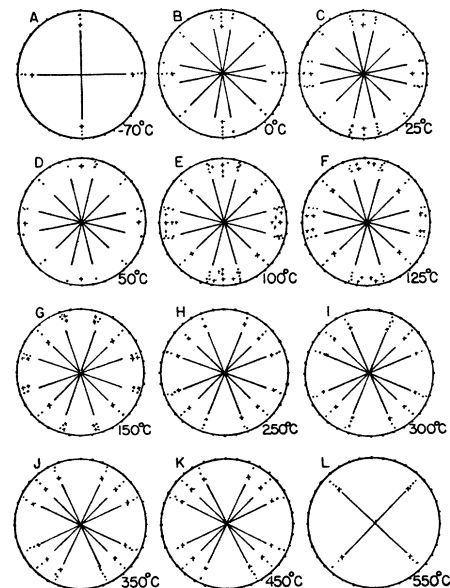


FIG. 4. Orientation of breakdown paths in LiF.

<sup>2</sup> A. von Hippel, *Zeits. f. Physik* **75**, 145 (1932); *Zeits. f. Elektrochemie* **39**, 506 (1933).

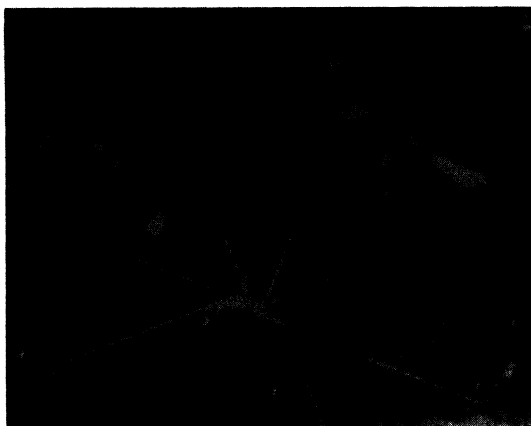


FIG. 5. Negative star in LiF at 300°C.

with increase of temperature than in LiF until they attained an azimuth of about 30° at 200°C. Thereafter the azimuth no longer changed with increase of temperature and hence LiCl did not yield [111] paths at elevated temperatures. The paths in LiCl showed a more pronounced tendency than in LiF to bend near the electrode and to give a wider spread of breakdown directions at constant temperature.

#### Lithium Bromide

The behavior of breakdown paths in LiBr is shown in Fig. 8:

(8A) At -170°C [110] dominant for d.c. and pulse. Paths appeared also at an azimuth of 15°.

(8B) At -60°C [110] dominant.

(8C) At 25°C average azimuth of 12° for d.c. and pulse.

(8D) At 100°C, pulse, (+) and (-), a 25° star (azimuth varied from 20° to 30°).

(8E) At 150°C a 30° star pattern was formed. The paths began to show a lack of definiteness in orientation and from time to time paths of lower azimuth appeared. Direct current yielded random dendrites.

(8F) At 200°C and above only stunted patterns of Fig. 6 were formed. A maximum azimuth of about 35° has been observed.

The behavior of breakdown paths in LiBr was very similar to that of LiCl.

#### RESULTS FOR OVERVOLTAGE

The patterns considered above were obtained under voltage conditions just sufficient for break-

down path formation. We know from the work of von Hippel<sup>2</sup> that path directions will change if excessive voltage is applied. Such overvoltage was produced by three methods: (1) as single pulses from the pulse generator described above; (2) as rectified voltage pulses from a leak tester that was drawn rapidly over the crystal surface; (3) as excess d.c. voltage on a probe which was lowered through oil towards the sample until breakdown occurred.

The overvoltage patterns obtained differed in complexity but showed the same sequence of path transitions. The most complex patterns were obtained in LiCl and LiBr by method (2). The (100) projection of a typical one is shown in Fig. 9, the thermal dependence of the patterns in Table I. The transformations involved only the off-diagonal paths. An initial star was formed whose azimuth increased with decrease of temperature. This star transformed abruptly into the [110], or nearly [110], directions and these in turn transformed into a 30° star. The 30° paths usually transformed by means of a smooth curve in LiBr (Fig. 10) or by discontinuous jumps yielding a spider leg-like pattern in LiCl into the orientation of normal breakdown.

When methods (1) and (3) were used, the overvoltage pattern always began at a later stage of development than in the above. A star with an azimuth in excess of that of normal breakdown, but not exceeding 30°, usually reduced azimuth smoothly in LiBr and discontinuously in LiCl until the normal breakdown direction was attained. In LiF overvoltage frequently yielded [111] paths at room temperature



FIG. 6. Typical heat degeneration of 30° patterns in LiCl and LiBr.

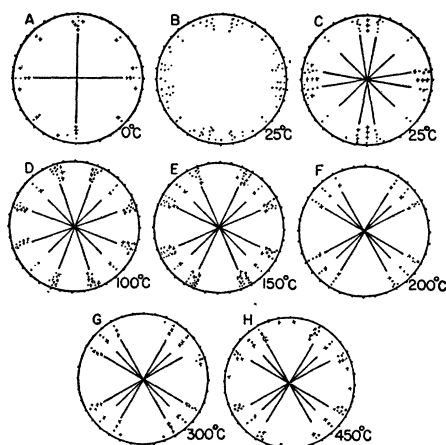


FIG. 7. Orientation of breakdown paths in LiCl.

and above; whereas in LiCl and LiBr  $[111]$  paths were never observed under normal conditions and with excess voltage only at  $-170^{\circ}\text{C}$  in conformity with the orientation of the initial star with temperature. LiF does, however, exhibit a discontinuous reduction in azimuth from  $30^{\circ}$  to normal breakdown as shown in Table I.

#### METALLIC DENDRITES

Dendrites were first observed by von Hippel<sup>3</sup> in the alkali halide crystals. They constitute a metallic (Na metal in NaCl, etc.) extension of the cathode within the crystal. The metallic growths, which form when moderate d.c. fields are impressed at elevated temperatures, frequently assume a definite crystallographic orientation; thus  $[111]$  dendrites appear in NaF,  $[100]$  and  $[110]$  in NaCl, etc.

In the lithium halide crystals the dendrites seemed to form at lower temperatures than in the other alkali halide crystals. In LiF they appeared (Fig. 11) as delicate pink growths resembling sea weed. Their intricate structure, which distinguishes them from the dendrites in the other alkali halides, may be due to a tendency to grow along star path directions. In general, it was not possible to assign lattice directions to the structure because it grows by the formation of a series of blobs, but, at times, a definite  $[110]$  orientation was noticed. All the dendrites grew (slowly compared with breakdown paths) from the cathode even when the point electrode was

rendered positive. Frequently the dendrites which were formed under excess d.c. voltage conditions terminated in breakdown paths as they approached the anode surface.<sup>3</sup>

Von Hippel has concluded<sup>4</sup> that the dendrites are probably electronic and not electrolytic in origin. It is thus possible that the dendrites and breakdown paths were formed by similar processes. It is of interest to note that the orientation of dendrites and breakdown paths was not necessarily the same at a given temperature.

#### SUPPLEMENTARY OBSERVATIONS ON RELATED CRYSTALS

##### Sodium Chlorate

It was shown previously<sup>1</sup> that sodium chlorate also yields star patterns. This crystal belongs to a different symmetry class and possesses a more complex structure than the lithium halides. The following results were obtained: at  $200^{\circ}\text{C}$  in 3 samples for (+) and (-) voltage precise star patterns of azimuth  $18^{\circ}$ ; at  $100^{\circ}\text{C}$  and at  $25^{\circ}\text{C}$  a star of azimuth  $22.5^{\circ}$ ; at  $-60^{\circ}\text{C}$  and at  $-170^{\circ}\text{C}$   $[111]$  paths at an azimuth of  $45^{\circ}$ , also paths at azimuths  $12^{\circ}$ ,  $18^{\circ}$ , and  $22.5^{\circ}$ . Inclination angle measurements show that the paths observed were again of the type  $[xxy]$  with  $x \geq y$  to an accuracy of  $3^{\circ}$ .

##### Sodium Fluoride

The path orientation in LiF with increasing temperature is represented by the scheme:

$$[110] \rightarrow [xxy] \rightarrow [111].$$

This behavior is at variance with the results obtained in NaF<sup>1</sup> which showed the  $[111]$  paths

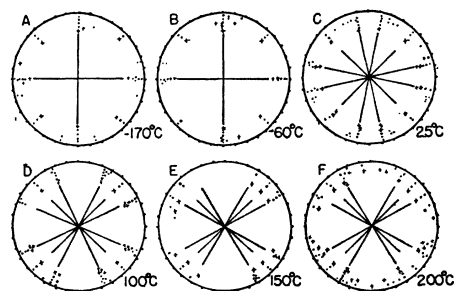


FIG. 8. Orientation of breakdown paths in LiBr.

<sup>3</sup> A. von Hippel, Zeits. f. Physik 98, 580 (1936).

<sup>4</sup> A. von Hippel, J. App. Phys. 8, 829 (1937).

TABLE I. Overvoltage patterns.

I. LiBr (+) and (-)	
(-170°C)	45°[111] paths
(25°C)	23°→0°→30°→12°
(100°C)	20°→0°→30°→22°
(150°C)	13°→0°→32°→28°
(300°C)	0°→30°
II. LiCl (+) and (-)	
(25°C)	10°→30°→17°→10°→18°
(25°C)	18°→0°→30°→0°
(100°C)	14°→0°→30°→12°→17°
III. LiF (-)	
(25°C)	30°→15°→0°→9°→12°
Azimuth 0° = [110]	

at low and the [110] paths at high temperature. The orientation of the paths in NaF as a function of temperature was therefore rechecked and confirmed.

For both polarities the tendency of breakdown path orientation in NaF changed from [111] at -170°C to [110] at 200°C. The [110] paths were still observed at 700°C. In spite of numerous tests in the intermediate temperature range, no indication of star paths was noticed; in every case both [111] and [110] paths were observed. With overvoltage, especially of negative sign, [100] paths accompanied by incipient (100) cleavage fractures were obtained at all temperatures investigated.

### Cesium Chloride

Below 450°C cesium chloride has a body-centered cubic lattice. The dominant breakdown

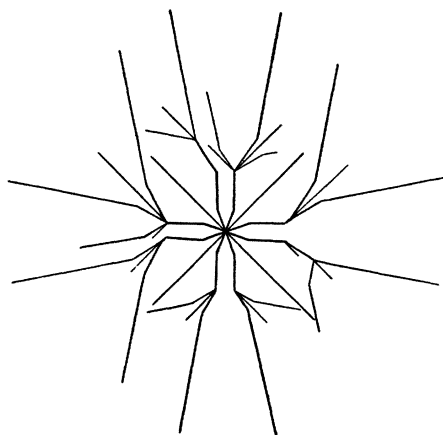


FIG. 9. (001) projection of the overvoltage pattern in LiCl at 25°C.

direction from -170°C to the transition temperature proved to be [111]; in addition, with overvoltage, [100] paths were observed.

### DISCUSSION

The experimental results presented in this and in the preceding paper<sup>1</sup> show that all the face-centered alkali halide crystals exhibit a thermal dependence of breakdown path orientation. All the halide salts of a given alkali atom show the same type of transformation. Except in the lithium halides the paths are confined to the three basic directions [100], [110], and [111]. In addition, random paths are observed at low temperatures in salts with low lattice energies.

The general behavior of breakdown paths may conform to the following mechanism.<sup>5</sup> Assuming that the paths result from local melting of the crystal by electronic avalanches, they mark those directions for which the conduction electrons can most readily be accelerated by the applied field to ionizing velocities. These directions will depend upon the interaction of the electronic wave-length and charge with the lattice. In a given direction the periodic lattice alternately transmits and reflects an electron as its velocity increases. Conversely, for a given wave-length the lattice is transparent in some directions and reflecting in others. During acceleration, since the wave-length is changing, first one and then another direction will become transparent, and the direction finally observed is the one in which the electron moved the greatest distance

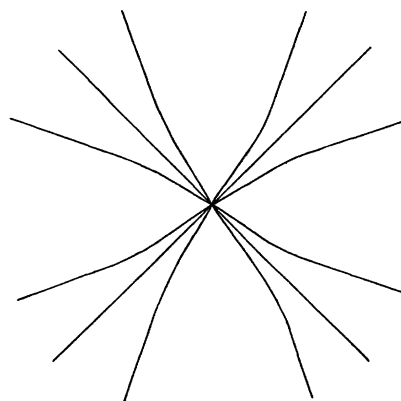


FIG. 10. Reduction of 30° star LiBr 25°C.

<sup>5</sup> A. von Hippel, Trans. Faraday Soc. 42A, 78 (1946).

between the ionization acts. Under normal breakdown we may expect to observe only one direction at each temperature, but with excess voltage a sequence of directions would be expected. The results obtained with overvoltage suggest that the patterns correspond to a deceleration of fast electrons near the probe into the crystal, since the final orientation corresponds to that of normal breakdown. In a sense the path directions mark the converse of Brillouin zones, because the zones represent regions of total reflection.

If the above mechanism is correct, it would seem that the star paths do not correspond to directions which may be derived by a simple wave interaction picture. One notices that the three basic breakdown directions  $[100]$ ,  $[110]$ , and  $[111]$  correspond to the three largest interplanar spacings or the three shortest interatomic distances in the lattice. If higher order paths are observed, the types  $[102]$ ,  $[112]$ , and  $[123]$ , etc. would be next in line in the sequence of interplanar spacings. However, only paths of the type  $[xxy]$  where  $x \geq y$  were observed and none of the above fall into this category.

It is possible to account for the geometrical locus of the patterns in the lithium halide crystals by assuming, as von Hippel has suggested,<sup>†††</sup> that the star paths may result from a competition in breakdown between the  $[110]$  and  $[111]$  directions. Because the distance between ionizing impacts may be very short, a statistical average direction would be observed macroscopically.

According to such a mechanism of competition the path orientation should follow a simple statistical distribution law. A careful examina-

<sup>†††</sup> In discussion with the writer.

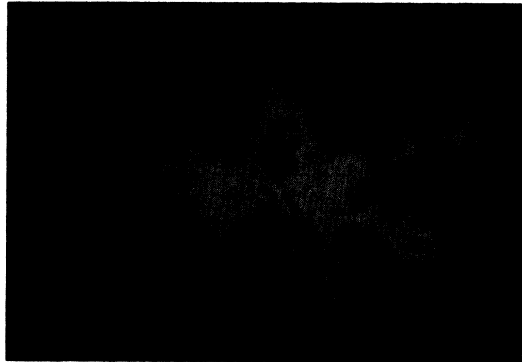


FIG. 11. Metallic dendrites in LiF at 200°C.

tion of the (+) breakdown paths in LiF at 25°C, however, did not show this. A count of paths in six crystal sections placed less than 1 path in 100 of those not falling in  $[110]$  directions at azimuths between 1° and 9°. Most of the paths lay between 10° and 13° and a few appeared at greater azimuths, while on a statistical basis one would expect paths at all angles from 0° to 13°. The orientations observed in the overvoltage patterns, which are reproducible and which follow the same sequence in each of 8 branches, are also difficult to explain in terms of a statistical breakdown mechanism, but seem to reflect an underlying order.

It is hoped that further work may definitely establish the role of the star pattern in the breakdown process.

#### ACKNOWLEDGMENT

The author wishes to express his gratitude to Professor Arthur von Hippel for his interest and advice throughout the course of this work.



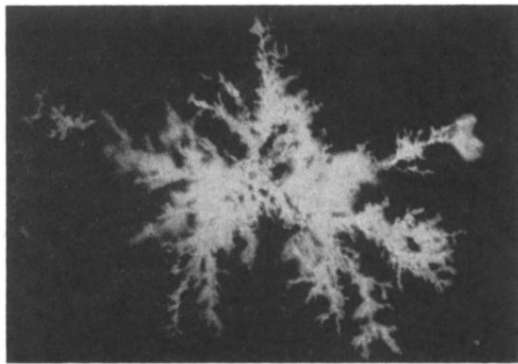


FIG. 11. Metallic dendrites in LiF at 200°C.

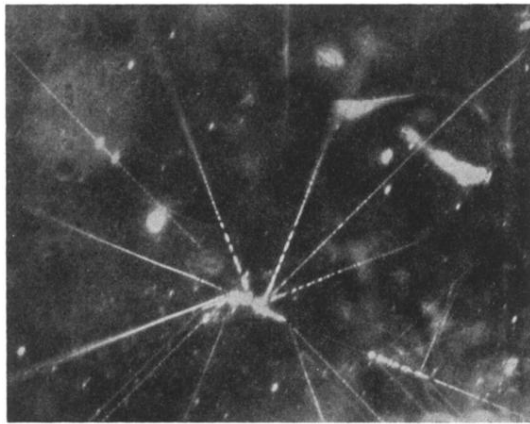


FIG. 5. Negative star in LiF at 300°C.

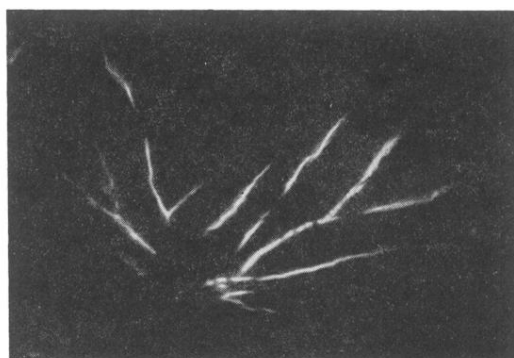


FIG. 6. Typical heat degeneration of  $30^\circ$  patterns in LiCl and LiBr.